ARTICLE
Journal of Cellular Biochemistry 115:290–302 (2014)

Journal of Cellular Biochemistry

# Human Wharton's Jelly Stem Cells and Its Conditioned Medium Enhance Healing of Excisional and Diabetic Wounds

Chui-Yee Fong,[1]* Kimberley Tam,[1] Suganya Cheyyatraivendran,[1] Shu-Uin Gan,[2] Kalamegam Gauthaman,[1] Arunmozhiarasi Armugam,[3] Kandiah Jeyaseelan,[3] Mahesh Choolani,[1] Arijit Biswas,[1] and Ariff Bongso[1]**

[1]*Department of Obstetrics and Gynaecology, Yong Loo Lin School of Medicine, National University Health System, National University of Singapore, Singapore 119228, Singapore*

[2]*Department of Surgery, Yong Loo Lin School of Medicine, National University Health System, National University of Singapore, Singapore 119228, Singapore*

[3]*Department of Biochemistry, Yong Loo Lin School of Medicine, National University Health System, National University of Singapore, Singapore 119228, Singapore*

## ABSTRACT

Wound healing is a major problem in diabetic patients and current treatments have met with limited success. We evaluated the treatment of excisional and diabetic wounds using a stem cell isolated from the human umbilical cord Wharton's jelly (hWJSC) that shares unique properties with embryonic and adult mesenchymal stem cells. hWJSCs are non-controversial, available in abundance, hypo-immunogenic, non-tumorigenic, differentiate into keratinocytes, and secrete important molecules for tissue repair. When human skin fibroblasts (CCD) in conventional scratch-wound assays were exposed to hWJSC-conditioned medium (hWJSC-CM) the fibroblasts at the wound edges migrated and completely covered the spaces by day 2 compared to controls. The number of invaded cells, cell viability, total collagen, elastin, and fibronectin levels were significantly greater in the hWJSC-CM treatment arm compared to controls ($P < 0.05$). When a single application of green fluorescent protein (GFP)-labeled hWJSCs (GFP-hWJSCs) or hWJSC-CM was administered to full-thickness murine excisional and diabetic wounds, healing rates were significantly greater compared to controls ($P < 0.05$). Wound biopsies collected at various time points showed the presence of green GFP-labeled hWJSCs, positive human keratinocyte markers (cytokeratin, involucrin, filaggrin) and expression of ICAM-1, TIMP-1, and VEGF-A. On histology, the GFP-hWJSCs and hWJSC-CM treated wounds showed reepithelialization, increased vascularity and cellular density and increased sebaceous gland and hair follicle numbers compared to controls. hWJSCs showed increased expression of several miRNAs associated with wound healing compared to CCDs. Our studies demonstrated that hWJSCs enhance healing of excisional and diabetic wounds via differentiation into keratinocytes and release of important molecules. J. Cell. Biochem. 115: 290–302, 2014. 

**KEY WORDS:** HUMAN WHARTON'S JELLY STEM CELLS (hWJSCs); hWJSC CONDITIONED MEDIUM; WOUND HEALING; SCRATCH-WOUND ASSAY; XENOGRAFT MURINE MODEL; EXCISIONAL AND DIABETIC WOUNDS

The skin is the largest organ covering the human body and is most prone to injury. The healing quality of surgical wounds vary, dehiscent wounds take a long time to heal and non-healing wounds are a chronic problem in patients suffering from diabetes,

All authors have no conflict of interests.

Grant sponsor: National Research Foundation (NRF), Proof-of-Concept grant:; Grant number: R-174-000-139-281; Grant sponsor: Academic Research Fund, National University of Singapore (AcRF-NUS); Grant number: R-174-000-129-112.

* Correspondence to: Dr. Chui-Yee Fong, Department of Obstetrics and Gynaecology, Yong Loo Lin School of Medicine, National University Health System, National University of Singapore, Kent Ridge, Singapore 119228, Singapore. E-mail: obgfong@nus.edu.sg

**Correspondence to: Dr. Ariff Bongso, Department of Obstetrics and Gynaecology, Yong Loo Lin School of Medicine, National University Health System, National University of Singapore, Kent Ridge, Singapore 119228, Singapore. E-mail: obgbongs@nus.edu.sg

Manuscript Received: 14 August 2013; Manuscript Accepted: 20 August 2013

Accepted manuscript online in Wiley Online Library (wileyonlinelibrary.com): 29 August 2013

DOI 10.1002/jcb.24661 • © 2013 Wiley Periodicals, Inc.

kidney failure, burns, and bed sores. Diabetic wounds lead to foot ulcers which eventually end up in lower limb amputations. Current methods such as chemicals, dressings, and skin grafts have been used to accelerate wound healing with limited success.

Reconstitution of damaged skin is a coordinated process involving the interplay and organization of multiple inflammatory cell types. However, studies on wound healing in PU.1 knockout mice which lack macrophages and neutrophils showed that neither of these cell types was important for wound healing [Martin et al., 2003]. The inherent physiological repair mechanisms become inefficient in the presence of (i) extensive loss of skin, (ii) pre-existing pathological diseases, (iii) superimposed microbial infections, (iv) impairment of local circulation, and (v) the presence of a foreign body [Mathieu et al., 2006]. The epidermis and skin appendages are renewed constantly and cell turnover is under the control of mesenchymal stem cells (MSCs) native to the epidermis, the hair bulb, the melanocyte layer, and the basal dermal layer [Badiavas et al., 2003]. It has also been shown that MSCs migrate from the bone marrow to the injured wound site and contribute to wound repair and regeneration [Borue et al., 2004; Sasaki et al., 2008]. MSCs assist these processes via four mechanisms (suppression of inflammation, angiogenesis, stimulation of stem cell proliferation, and differentiation into new keratinocytes by dying apoptotic cells) [Jackson et al., 2012]. The administration of an exogenous source of MSCs to wounds therefore is an attractive form of potential therapy. The MSCs that have been traditionally used are those from the human bone marrow (hBMMSCs) from autologous and allogeneic sources. Some basic mechanisms have been suggested to explain how these MSCs repair tissues but these mechanisms have not been studied in-depth and confirmed. The hypotheses are (i) the creation of an environment that enhances regeneration of endogenous cells and (ii) differentiation of the MSCs into keratinocytes [Stoff et al., 2009]. Several groups have reported successful wound healing after administration of hBMMSCs to surgical wounds [Chen et al., 2009; Stoff et al., 2009], diabetic wounds [Kuo et al., 2011] and burns [Bey et al., 2010]. Unfortunately, the use of hBMMSCs has its limitations such as the problems of painful harvest, low cell numbers, risk of infection and morbidity. Primary hBMMSCs also lose their stemness properties after a few passages in vitro compromising on the availability of large numbers for clinical application. Alternative sources of stem cells are being explored.

We and others have studied a stem cell from the human umbilical cord Wharton's jelly (hWJSCs) that shares unique properties between embryonic and adult stem MSCs [Troyer and Weiss, 2008; La Rocca et al., 2009; Bongso and Fong, 2013]. These cells have low-level expression of embryonic stem cell markers and satisfy the criteria recommended by the International Society of Cytotherapy for MSCs [Dominici et al., 2006]. Genomic, cell behavior, and stemness characterization studies [Troyer and Weiss, 2008; Fong et al., 2011; Bongso and Fong, 2013] showed that hWJSCs are primitive MSCs with uniquely different properties from bone marrow and other MSCs. These differences were attributed to their umbilical cord origin which embryologically lies in between embryonic and adult tissues on the human developmental map [Pappa and Anagnou, 2009]. It was reported that during early human development primitive MSCs migrate from the aorta-gonad-mesonephros (AGM) of the embryo through the umbilical cord to the placenta and then migrate back again through the umbilical cord to home in the liver and bone marrow of the fetus [Wang et al., 2008]. It was suggested that *en route* these primitive MSCs get trapped in the gelatinous Wharton's jelly of the umbilical cord, reside there and acquire unique characteristics in their new environment [Taghizadeh et al., 2011]. Such primitive hWJSCs are not exposed to the insults of the adult environment and may thus have implications in the absence of scar formation in the fetus during pregnancy. Interestingly, abdominal hernias in newborn infants have been successfully treated by attaching the infant's own umbilical cord to the hernia with no ensuing scar formation [Lorenz et al., 1992; Estes et al., 1993].

The advantages of hWJSCs over other stem cells include their (i) non-controversial nature, painless harvest, availability in large numbers and ability to differentiate into keratinocytes, (ii) prolonged stemness properties in vitro (iii) tolerance in donor settings, and (iv) anti-tumorigenicity [Fan et al., 2011; Gauthaman et al., 2012]. Additionally, they are proliferative and hence can be scaled up in large numbers for clinical application and several studies have shown that they are safe and do not induce tumor formation in both laboratory animals [Fan et al., 2011; Gauthaman et al., 2012] and non-human primates [Wang et al., 2012]. We report here the evaluation of hWJSCs and its conditioned medium (hWJSC-CM) in wound healing using conventional in vitro scratch-wound migration assays and in vivo full-thickness excisional and diabetic wounds created in immunodeficient and diabetic mice. Since skin cell turnover is under the control of MSCs this was the theoretical basis for this study.

## MATERIALS AND METHODS

### ETHICAL APPROVAL FOR USE OF HUMAN CELLS AND ANIMALS

Ethical approval with informed patient consent for the use of human umbilical cords for this study was given by the Institutional Domain Specific Review Board (DSRB), Singapore. hWJSCs were derived, propagated, and characterized according to our earlier published protocols [Fong et al., 2007; Fong et al., 2010]. Commercial skin fibroblasts (CCD-1112 sk) (abbreviated as CCD) were purchased from the American Type Culture Collection (ATCC, Rockville, MD) and ethical approval for their use was given by the National University of Singapore, Institutional Review Board (NUS-IRB). All animal procedures were approved by the National University of Singapore Institutional Animal Care and Use Committee (IACUC).

### CELL CULTURE

Umbilical cords were collected at full term delivery in transport medium (Hank's Balanced Salt Solution supplemented with antibiotic–antimycotic solution, Invitrogen Life Technologies, Carlsbad, CA), stored at 4°C and processed within 12 h after collection. Each cord was cut first into 2 cm pieces and each of the pieces cut open lengthwise and placed with its inner surface facing down in a 60 mm Petri dish containing an enzymatic solution. The enzymatic solution comprised of 2 mg/ml collagenase type I, 2 mg/ml collagenase type IV, and 100 IU/ml hyaluronidase (Sigma, St Louis, MO) in DMEM High glucose medium (Invitrogen). The umbilical blood vessels were not

removed. The dishes were then incubated at 37°C for 30–45 min to facilitate detachment and loosening of the Wharton's jelly into culture medium. The gelatinous Wharton's jelly was then collected into sterile syringes and the hWJSCs then separated from the Wharton's jelly by syringing the gelatinous masses through a hypodermic needle. The isolated hWJSCs were cultured in sterile tissue culture flasks [Becton Dickinson (BD) Franklin Lanes, NJ] using hWJSC culture medium comprising of DMEM-high glucose medium supplemented with 20% fetal bovine serum (FBS), 16 ng/ml basic fibroblast growth factor (Millipore Bioscience Research agents, Temecula, CA), 1% non-essential amino acids, 2 mM L-glutamine, 0.1 mM β-mercaptoethanol, 1% insulin–transferrin–selenium and 1% antibiotic–antimycotic mixture [penicillin (100 units/ml), streptomycin (100 μg/ml), and amphotericin B (0.25 μg/ml)] (Invitrogen).

The commercial frozen CCDs were thawed and cultured in sterile tissue culture flasks (BD) in DMEM-high glucose medium supplemented with 10% FBS, 2 mM L-glutamine and antibiotic–antimycotic mixture.

After establishment of confluent monolayers the hWJSCs and CCDs were detached from the plastic dishes with a dissociation reagent (TrypLE™ Express, Invitrogen), washed and seeded on 0.1% gelatin-coated tissue culture plates in a basal medium devoid of proteins comprised of DMEM-high glucose, 10% knockout serum replacement (KOSR), 1% L-glutamine and 1% antibiotic–antimycotic mixture (KOSR medium, Invitrogen) for the in vitro experiments and DMEM-high glucose, 1% L-glutamine and 1% antibiotic–antimycotic mixture for the in vivo experiments of the present study. A protein-free basal medium was used in both in vitro and in vivo studies so as to take advantage of the various proteins released by the hWJSCs and CCDs.

### LABELING OF hWJSCs WITH GREEN FLUORESCENCE PROTEIN (GFP)

The hWJSCs were infected with a lentiviral vector for GFP. Briefly, lentiviral vectors were produced by transient transfection of Lenti-X™ 293T Cells (Clontec Laboratories, Inc., Mountain View, CA). hWJSCs ($5 \times 10^6$ cells/plate) were seeded in 10 cm tissue culture plates 24 h before transfection. Transfection was performed using the calcium phosphate precipitation method. Cells were replaced with fresh medium at 14–16 h after transfection. The supernatant was filtered through a 0.45 mm filter and the titer of the supernatant of the 293T cells was determined using flow cytometry. The hWJSCs were infected with unconcentrated lentiviral supernatant at a multiplicity of infection (MOI) of 5–10.

### CONDITIONED MEDIUM

hWJSCs and CCDs at passages 3–4 (P3–P4) were grown to 80% confluence in KOSR medium and the medium separated after 72 h as hWJSC conditioned medium (hWJSC-CM) and CCD conditioned medium (CCD-CM), respectively. The conditioned media were filter-sterilized using a 0.22 μm Millex-GP syringe filter (Millipore, Billerica, MA) and the pH and osmolality of the media standardized before use in experiments. The mean ± SEM pH and osmolality of the hWJSC-CM and CCD-CM were 7.75 ± 0.26 and 332.67 ± 1.20 and 7.88 ± 0.18 and 332.33 ± 0.88, respectively. Both hWJSC-CM and CCD-CM were diluted 1:1 v/v in KOSR medium and used as 50% hWJSC-CM and 50% CCD-CM for all experiments. Our previously published work on the composition of hWJSC-CM showed that it contained a family of cytokines, growth factors, glycosoaminoglycans, and cell adhesion molecules [Fong et al., 2012; Gauthaman et al., 2012].

### SCRATCH-WOUND ASSAY

Several dishes were prepared using the same batch of CCDs for conventional scratch-wound assays according to the method of Cory [2011]. Briefly, CCDs were cultured in KOSR medium at a seeding density of $0.5 \times 10^6$ cells on 0.1% gelatin-coated 60 mm Petri dishes (Nalgene NUNC International, Rochester, NY) and incubated at 37°C in a 5% $CO_2$ in air atmosphere for 24 h to generate confluent monolayers. Linear scratches (0.5 mm width) were made vertically from top to bottom in the midline of the confluent CCD monolayers using a sterile pipette. The scratched dishes were then divided into one treatment arm (hWJSC-CM) and two controls [CCD-CM and unconditioned KOSR medium (UCM)]. The scratched dishes were seeded with 2 ml of hWJSC-CM, CCD-CM, and UCM, respectively. All treatment and control dishes were then incubated at 37°C in a 5% $CO_2$ in air atmosphere for 72 h. CCD migration and number of invading cells into the scratches were evaluated according to the protocols of Jeon et al., [2010]; Walter et al., [2010], and Kim et al., [2012]. Briefly, CCD migration into the vacant scratches was monitored regularly and digitized images of at least five random fields (0.6 $mm^2$ area) within the scratches were taken every 24 h using inverted phase contrast optics until 72 h or full closure of the scratches. Markings on the Petri dishes were used as reference points to monitor the same fields every 24 h. The mean ± SEM number of invaded CCDs into the scratches at 24, 48, and 72 h were calculated [Jeon et al., 2010; Walter et al., 2010; Kim et al., 2012]. The MTT assay was used to calculate viable CCD numbers to find out whether the respective treatments had stimulated the proliferation of live CCDs. The MTT assay was carried out using a MTT reagent kit [3-(4, 5-dimethylthiazolyl-2)-2, 5-diphenyltetrazolium bromide] (Sigma) according to the manufacturer's instructions. Absorbance at 570 nm was spectrophotometrically measured using a microplate ELISA reader (μQuant-BioTek, Winooski, VT) with a reference wavelength of 630 nm. Three replicates were carried out for each assay.

### SIRCOL (COLLAGEN) AND FASTIN (ELASTIN) ASSAYS

The total collagen (Types I–V) and elastin levels of CCDs in the treatment and control arms were evaluated and compared using the Sircol™ (collagen assay) and Fastin™ (Elastin assay) kits (Bioclour, Carrickfergus, UK) according to the manufacturer's instructions. Absorbance at 555 nm was spectrophotometrically measured using a microplate ELISA reader (μQuant-BioTek) and collagen concentration calculated based on the concentration of the standards.

### QUANTITATIVE REAL TIME POLYMERASE CHAIN REACTION (qRT-PCR)

CCDs exposed to treatment and control arms were subjected to qRT-PCR. Total RNA was extracted using TRIzol™ reagent (Invitrogen). RNA quality and quantity were measured using a Nanodrop™ spectrophotometer (Nanodrop Technologies, Wilmington, DW) and all samples were treated with DNase-I prior to first strand cDNA synthesis with random hexamers using the SuperScript™ first strand

synthesis system (Invitrogen). Primer sequences were taken from earlier published studies and are given in Table I. qRT-PCR analysis was performed with the ABI PRISM 7500 Fast Real-Time PCR System (Applied Biosystems, Foster City, CA) using SYBR green as previously described and relative quantification was performed using the comparative $C_T$ ($2^{-\Delta\Delta CC_T}$) method.

### FULL THICKNESS WOUND MODEL IN SCID AND DIABETIC MICE

For the evaluation of hWJSCs or hWJSC-CM on the healing of excisional wounds a total of 45 female severely combined immunodeficient (SCID) mice aged 5–6 weeks were obtained from the Animal Resources Centre, Western Australia. After the mice were allowed acclimatization for a week they were anesthetized using isofluorane, dorsal regions shaved, and two 8-mm full-thickness circular wounds created on left and right dorsal sides using a dermal punch (Accusharp Punch, India). All mice were co-administered with 2 mg/kg bupivacaine (local anesthesia) together with isofluorane prior to wound punch. Following 3 days post-surgery, the mice were administered with 0.05 mg/kg buprenorphine twice a day subcutaneously. All wounds were covered with Tegaderm (3 M) and edges sealed with Dermabond™ (Ethicon). Dermabond™ helps in preventing the mice removing the Tegaderm plaster and is an FDA approved adhesive that forms a protective barrier against bacteria. The 45 mice (90 wounds) were divided into five groups (nine mice/group; 18 wounds) and the wounds in each group treated as follows [Gp 1 (Treatment): GFP-hWJSCs ($1 \times 10^6$ cells in 100 μl PBS); Gp 2 (Treatment): hWJSC-CM (100 μl); Gp 3 (Control): GFP-CCDs ($1 \times 10^6$ cells in 100 μl PBS); Gp 4 (Control): CCD-CM (100 μl) and Gp 5 (Control): Unconditioned medium (UCM) (100 μl)]. The cells and media were administered intradermally using a 25 G hypodermic needle at several sites at the margins of the wounds. The animals were individually housed under a 12:12 h light–dark cycle, under SPF conditions and allowed access to food and drinking water.

For the diabetic wound evaluation, a similar experimental design as above was carried out on full-thickness (6 mm) wounds created in diabetic mice (Strain BKS.Cg-Dock7$^m$ +/+*Lepr$^{db}$*/J; Stock No: 000642 resembling Type IIDM) obtained from Jackson Laboratories, USA. A smaller sized wound punch was chosen for the diabetic wounds to simulate other published murine diabetic wound healing studies [Sullivan et al., 2004; Wu et al., 2007]. Glucose levels were measured before, during, and after the experiment to confirm that the mice were diabetic. A total of 36 mice (72 wounds) were divided into three groups (12 mice/group; 24 wounds) and the diabetic wounds in each group treated as follows: [Gp 1(Treatment): GFP-hWJSCs ($1 \times 10^6$ cells in 100 μl PBS); Gp 2 (Treatment): hWJSC-CM (100 μl); Gp 3 (Control): UCM (100 μl)]. Injections were administered intradermally using a 25 G hypodermic needle at several sites at the margins of the wounds.

Wound healing was visually monitored and documented daily in the excisional and diabetic wound groups of mice. Digital photographs were taken on days 0, 7, and 14 for excisional and diabetic wounds by the same operator. The percentage healing rates were calculated from the digital images using a NIH recommended formula and Image software by two independent observers blinded to treatments. The formula used was as follows: (original wound area − new wound area)/original wound area × 100 [Chen et al., 2009].

At specific time points, animals were culled and the entire wound, including a margin of approximately 2 mm of unwounded skin, was excised down to the fascia and removed. The excised "wound" samples were divided equally into two halves for (i) snap-freezing for cryostat sectioning for fluorescent microscopy and immunohistochemistry analysis and (ii) RNA extraction. The other wound on the opposite side was also divided into equal halves for (iii) histological analysis, and (iv) snap-freezing for molecular analysis. Each of the analyses was carried out in a blinded fashion by staff experienced in these areas in their respective laboratories. For histology, at least 4–7 different sections were examined for each arm in treatment and control groups. Normal murine skin samples from SCID and diabetic mice were used as positive controls for comparison.

TABLE I. The ECM-Related Genes and Primer Sequences Used for qRT-PCR

| Gene | Primer sequence |
|---|---|
| GAPDH | F: 5′- GCACCGTCAAGGCTGAGAAC -3′<br>R: 5′- GGATCTCGCTCCTGGAAGATG -3′ |
| Collagen Type I | F: 5′- CACAGAGGTTTCAGTGGTTTGG -3′<br>R: 5′- GCACCAGTAGCACCATCATTTC -3′ |
| Collagen Type III | F: 5′- CTGAAATTCTGCCATCCTGAAC -3′<br>R: 5′- GGATTGCCGTAGCTAAACTGAA -3′ |
| Fibronectin | F: 5′- AAGATTGGAGAGAAGTGGGACC -3′<br>R: 5′- G GAGCAAATGGCACCGAGATA -3′ |

F, forward primer; R, reverse primer, GAPDH, glyceraldehyde-3-phosphate dehydrogenase.

### IDENTIFICATION OF GFP SIGNALS AND KERATINOCYTE MARKERS IN WOUND SAMPLES

The wound samples collected for fluorescent microscopy that were fixed in 4% buffered paraformaldehyde were washed in PBS for 24 h and perfused in 18% sucrose for 24 h. The samples were then mounted in Tissue-Tek® OCT Compound (Sakura Finetek USA, Inc., CA) and stored at −80°C. Cryosections (5 μm) were cut using a cryostat (CM1650; Leica, Germany) and mounted on glass slides coated with polysine (Thermo Scientific). The sections were exposed to a blocking solution of 10% normal goat serum and then incubated with mouse monoclonal anti-human filaggrin (Abcam, Cambridge, UK), anti-human involucrin (Genway, San Diego, MO), and anti-human cytokeratin (clone AE1/AE3) (Dako, Carpinteria, CA) overnight. The samples were then washed in PBS three times (10 min each time) and exposed to Cy3-conjugated secondary antibodies (Abcam) for 1 h. Finally, the samples were washed in PBS thrice and mounted with Fluoroshield™ with DAPI (Sigma) together with a cover slip. The sections were examined and photographed with a digital camera under a fluorescent microscope (Nikon Eclipse, Ti-S, Nikon Corporation, Tokyo, Japan) fitted with blue (DAPI), green (GFP), and red (Cy3) filters.

### GENE EXPRESSION ANALYSIS IN WOUND SAMPLES

Murine gene expression for VEGF-A, TIMP-1, and ICAM-1 in wound biopsies were analyzed by the Quantitative Real-Time PCR TaqMan method. Briefly, total RNA was isolated from treatment and control wound samples (n = 3 per arm), homogenized using TissueLyser LT (Qiagen) and a Universal Tissues EZ1 kit and used as a substrate (1 μg)

for reverse transcription using a High Capacity cDNA Reverse Transcription Kit (Applied Biosystems). TaqMan Fast Advance Mastermix (Applied Biosystems) was used for Fast Real-Time PCR. Quantification of VEGF-A expression was performed with the TaqMan Gene expression Assay (Applied Biosystems) for the target VEGF gene (Mm01281449_m1). Quantification of cytokine release (TIMP-1 and ICAM-1) was performed using quantitative real-time PCR. TaqMan Gene Expression Assays (Applied Biosystems) were used for the target genes TIMP-1 (Mm00441818_m1) and ICAM-1 (Mm00516023_m1). The endogenous reference genes (Mm99999915_g1) for GAPDH were used for quantitative real-time PCR.

### STATISTICAL ANALYSIS OF IN VITRO AND IN VIVO STUDIES

For the in vitro studies the differences observed between treatment and control groups were compared and analyzed using Student's *t*-test as recommended by Jeon et al., [2010] and Kim et al., [2012]. The results were expressed as mean ± SEM and a value of $P < 0.05$ was considered to be statistically significant. For the in vivo studies the results were expressed as mean ± SEM and analyzed by ANOVA and the post-hoc test with least-significant difference (LSD). Statistical significance was determined using SPSS software, version 13.0 (SPSS, Chicago) and *P* values of <0.05 were regarded as statistically significant.

### TOTAL RNA EXTRACTION AND MICROARRAYS

Total RNA (+ miRNA) was extracted from hWJSCs and CCDs by a single-step method using TRIzol reagent (Invitrogen) according to manufacturers' protocol. miRNA array was performed [Karolina et al., 2011] using total RNA (1 μg) which was 3′-end-labeled with Hy3 dye using the miRCURY LNA™ Power Labeling Kit (Exiqon, Denmark) and hybridized for 16–18 h on miRCURY LNA™ Arrays (MirBase version 16) using the MAUI® hybridization system. The microarray chips were then washed and scanned using an InnoScan700, microarray scanner (Innopsys, Carbonne, France) and analyzed on Mapix® Ver4.5 software.

The first stage of analysis on microarray data was performed using Partek® 6.6 Genomics Suite software (Copyright, Partek, Inc., St. Louis, MO). Briefly, background-subtracted median signal intensity of miRNAs was used for analysis. First stage of normalization was carried out against a group of endogenous controls and the spike-in controls for each chip to avoid technical and experimental variations for the hWJSCs and the CCD miRNA profiles. The normalized data was subjected to one-way ANOVA and the differentially regulated miRNAs were selected following Benjamini–Hochberg false discovery rate (FDR) correction. All statistical analysis was performed using the statistical tools provided by Partek® 6.6 Genomics Suite software.

## RESULTS

### GROWTH AND CHARACTERIZATION OF hWJSCs AND CCDs

In-house derived hWJSC and commercial skin fibroblast (CCD1112sk) (abbreviated as CCD) cell lines were successfully established and characterized before their use. When green fluorescent protein (GFP)-labeled hWJSCs and CCDs were cultured in a protein-free basal medium with knock-out serum replacement (KOSR medium) they adhered well to plastic, maintained their typical fibroblastic morphology and became confluent. The GFP-hWJSCs were positive for the CD signature markers (CD10, CD13, CD29, CD44, CD90), and satisfied the criteria for MSCs [Dominici et al., 2006]. They also had low-level expression of OCT4, NANOG, and SOX2.

### SCRATCH-WOUND ASSAY

The skin fibroblasts in scratch-wound assays when exposed to the hWJSC-CM treatment arm started to migrate from the edges of the scratches ("wounds") into the wound spaces as early as 6–8 h and then completely covered the spaces by day 2 (48 h) compared to controls [CCD conditioned medium (CCD-CM) and unconditioned KOSR medium (UCM)] (Fig. 1A). The mean ± SEM number of cells that had invaded the scratches as determined by two independent observers were significantly greater in the hWJSC-CM treatment arm compared to controls ($P < 0.05$) (Fig. 1B). The mean ± SEM cell numbers that migrated into the wound areas were 60 ± 04 (hWJSC-CM), 53 ± 06 (CCD-CM), and 48 ± 04 (UCM) at 24 h; 159 ± 13 (hWJSC-CM), 88 ± 05 (CCD-CM), and 92 ± 07 (UCM) at 48 h; and 276 ± 17 (hWJSC-CM), 142 ± 09 (CCD-CM), and 163 ± 12 (UCM) at 72 h, respectively. The viability of the CCDs (MTT assay) for the treatment arm (hWJSC-CM) was also significantly greater than the controls at 72 h (Fig. 1C).

### COLLAGEN AND ELASTIN (SIRCOL AND FASTIN ASSAYS)

The collagen and elastin concentrations using Sircol and Fastin assays, respectively, on CCDs were significantly greater in the treatment arm (hWJSC-CM) compared to the controls at 72 h. ($P < 0.05$) (Fig. 2A,B).

### COLLAGEN TYPE I, III, AND FIBRONECTIN (qRT-PCR)

qRT-PCR of the CCDs in the treatment arm (hWJSC-CM) showed significantly greater expression of collagen type I, collagen type III, and fibronectin compared to the controls (CCD-CM and UCM) ($P < 0.05$). The increase in gene expression of fibronectin for the hWJSC-CM arm was 300-fold compared to 40-fold for the CCD-CM arm. Collagen I and III were increased by 17- to 20-fold for the hWJSC-CM arm compared to three- to fourfold for the CCD-CM arm (Fig. 2C–E).

### HEALING RATES AND HISTOLOGY OF EXCISIONAL AND DIABETIC WOUNDS IN MICE

Macroscopic digitized images of healing of circular full-thickness murine excisional wounds after application of GFP-hWJSCs and hWJSC-CM (treatment arms) and CCD-CM and UCM (controls) showed that wound closure was greater in the treatment arms compared to controls (Fig. 3A). Wound healing rates using the wound healing formula on digital images recommended by Chen et al., [2009] showed that the GFP-hWJSCs and hWJSC-CM treatment groups exhibited significantly greater healing rates compared to all control groups (GFP-CCDs, CCD-CM, and UCM) on day 7 (Fig. 3B). On day 14, the GFP-hWJSCs treated wounds healed the greatest ($P < 0.05$) (Fig. 3B). Histological analysis of excisional wounds on day 14 showed that the epidermis and dermal layers of wound areas in the treatment groups (GFP-hWJSCs and hWJSC-CM) had increased reepithelialization, cellularity and vasculature, and increased sebaceous gland and hair follicle numbers compared to controls (Fig. 3C). On D7 even

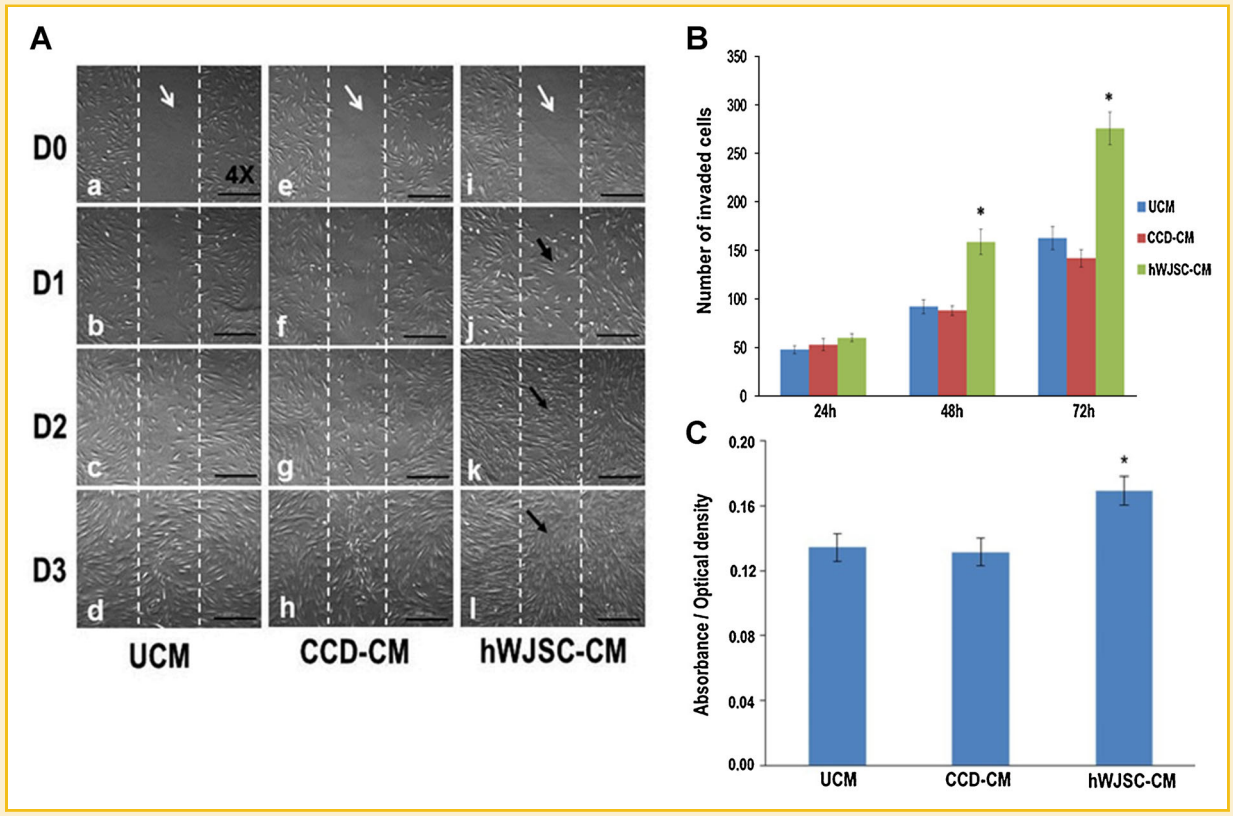


**Fig. 1.** A: Scratch-wound assay of CCD fibroblasts exposed to hWJSC-CM (0–72 h). a–d: CCD fibroblasts grown in unconditioned medium KOSR medium (UCM) (control); e–h: CCD fibroblasts grown in CCD-CM (control); i–l: CCD fibroblasts grown in hWJSC-CM (treatment). White arrows in (a), (e), and (i) indicate vertical scratches in middle of monolayer with no CCD fibroblasts at D0. Black arrows in (j), (k), and (l) show faster migration and increased numbers of CCDs into scratches in hWJSC-CM arm compared to controls. The scratches in the hWJSC-CM arm were fully closed by D2. B: The mean ± SEM number of invading cells into scratches were significantly greater in the hWJSC-CM arm compared to both controls at 48 and 72 h ($^*P < 0.05$). C: The mean ± SEM CCD viability (MTT assay) was significantly greater in the hWJSC-CM arm compared to both controls at 72 h ($^*P < 0.05$). Results are expressed as optical density values relative to controls.

though healing rates were not 100% in the hWJSCs and hWJSC-CM treatments arms, some histological sections showed both dermal and epidermal layers suggesting that the healing process was rapid.

Macroscopic observations, percentage healing rates and histology confirmed that healing of diabetic wounds was also significantly enhanced in GFP-hWJSCs and hWJSC-CM treated mice compared to controls over a 28-day period (Fig. 4A–C). On day 14 diabetic wounds appeared larger than day 7 wounds because db/db skin does not heal by the same contraction mechanisms as normal murine skin [Sullivan et al., 2004].

### GFP-HWJSC SURVIVAL AND DIFFERENTIATION INTO KERATINOCYTES IN MURINE EXCISIONAL AND DIABETIC WOUNDS

Engraftment and survival of GFP-hWJSCs in the excisional and diabetic wounds at days 14 and 28 were confirmed from green signals via immunofluorescence microscopy (Fig. 5). The number of GFP-hWJSCs in the wound biopsies gradually reduced with wound closure compared to the initial numbers applied to wounds. Immunohistochemistry of excisional and diabetic murine wound biopsies on days 14 and 28 showed the presence of positive human keratinocyte markers (cytokeratin, involucrin, and filaggrin) (Fig. 5).

### DIFFERENTIAL GENE EXPRESSION IN EXCISIONAL AND DIABETIC WOUNDS

On day 3 after initiation of wounds, ICAM-1 mRNA levels in excisional wounds in mice treated with GFP-hWJSCs were significantly higher than CCD-CM and GFP-CCDs arms ($P < 0.05$) (Fig. 6A). TIMP-1 expression was also significantly upregulated in excisional wounds on day 3 in the GFP-hWJSCs treatment arm compared to controls ($P < 0.05$) (Fig. 6A). Interestingly, VEGF-A mRNA expression on day 3 showed a sixfold increase when excisional wounds were exposed to hWJSC-CM ($P < 0.05$) (Fig. 6A). On day 7, both GFP-hWJSCs and hWJSC-CM treatment arms showed significantly greater ICAM-1, TIMP-1, and VEGF-A expression levels compared to controls in excisional wounds ($P < 0.05$). On day 14, the mRNA expression levels of ICAM-1 for excisional wounds were not significantly different between groups but VEGF-A levels remained significantly greater in GFP-hWJSCs and hWJSC-CM treatment arms compared to controls ($P < 0.05$) (Fig. 6A).

For diabetic wounds, the hWJSC-CM treatment arm showed significantly greater levels of TIMP-1 on days 7 and 14 and VEGF-A on days 7 and 28 compared to controls. VEGF-A levels for the

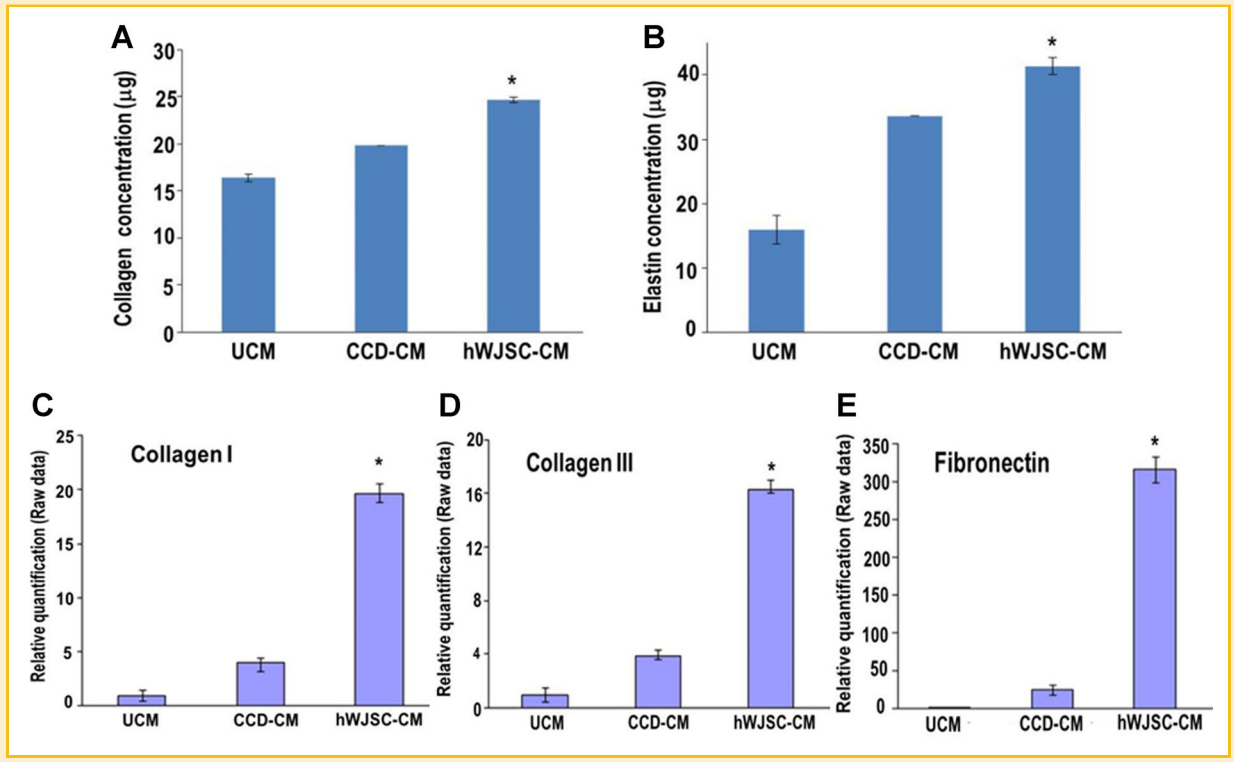


**Fig. 2.** A,B: The mean ± SEM levels of collagen (Sircol assay) and elastin (Fastin assay) of CCDs were significantly greater in the hWJSC-CM treatment arm compared to controls (*$P < 0.05$). C–E: qRT-PCR analysis showed significantly greater expression of (C) collagen type I, (D) collagen type III, and (E) fibronectin in the CCDs exposed to hWJSC-CM compared to controls (*$P < 0.05$). GAPDH was the internal control. Data analysis and relative quantitation were done using the comparative $C_t$ ($\Delta\Delta C_T$) method.

GFP-hWJSCs arm were significantly greater than controls in diabetic wounds on day 28 ($P < 0.05$) (Fig. 6B).

### miRNA PROFILE IN hWJSCs

Among the 487 miRNAs that were found to be differentially regulated between hWJSCs and CCDs, 82 miRNAs were expressed in hWJSCs at significantly higher levels (FDR, $P < 0.1$). Among them only hsa-miR-27a-5p, -98, -181a, -196a-3p, -374a, -601, -622, -920, -3915, and -3924 were found to be upregulated in hWJSCs. The remaining 72 miRNAs were downregulated in hWJSCs compared to CCDs. Nevertheless, several miRNAs that are involved in endothelial function and proliferation processes including wound healing were highly expressed in hWJSCs (Table II).

## DISCUSSION

Wound healing can be divided into three phases (1) inflammation, (2) proliferation, and (3) remodeling [Maxson et al., 2012]. During the proliferative phase native MSCs are recruited to differentiate into new keratinocytes and in the final remodeling phase endogenous dermal fibroblasts reorganize the extracellular matrix (ECM) to reinforce the granulation tissue [Jackson et al., 2012; Maxson et al., 2012]. It has been a long-held view that MSCs applied to wounds modulate the host wound environment by indirect mechanisms acting as a vector to deliver important therapeutic molecules.

In the present study the GFP-hWJSCs and hWJSC-CM arms showed significantly greater wound healing compared to controls suggesting that direct and indirect mechanisms of wound healing were taking place by directed differentiation of GFP-hWJSCs into keratinocytes and indirectly by the release of important bioactive molecules that initiate and facilitate the host response to tissue repair. Since the wound biopsies showed the survival of green GFP-hWJSCs signals and species-specific upregulation of human keratinocyte markers (cytokeratin, involucrin, and filaggrin), differentiation of the GFP-hWJSCs into new keratinocytes was probably helping reepithelialization in the excisional and diabetic wounds. Other workers have also shown that human umbilical cord MSCs differentiate into keratinocytes when administered locally into the wound beds of mice [Luo et al., 2010]. We and others have also observed that hWJSCs readily differentiate into keratinocytes in vitro using two conventional differentiation protocols [Schneider et al., 2010; Jin et al., 2011]. Cell proliferation is essential in the regenerative phase of wound healing and apart from the dermal fibroblasts and keratinocytes, the stem, or progenitor cells within the skin niches are also involved in cell turnover [Harris et al., 2012]. Our results are consistent with the findings of Shin and Peterson [2013] that the introduction of soluble bioactive molecules into wounds via the hWJSC-CM and secretion of the same molecules by the engrafted GFP-hWJSCs creates a niche for the recruitment of native skin MSCs and progenitor cells to the wound site to facilitate healing.

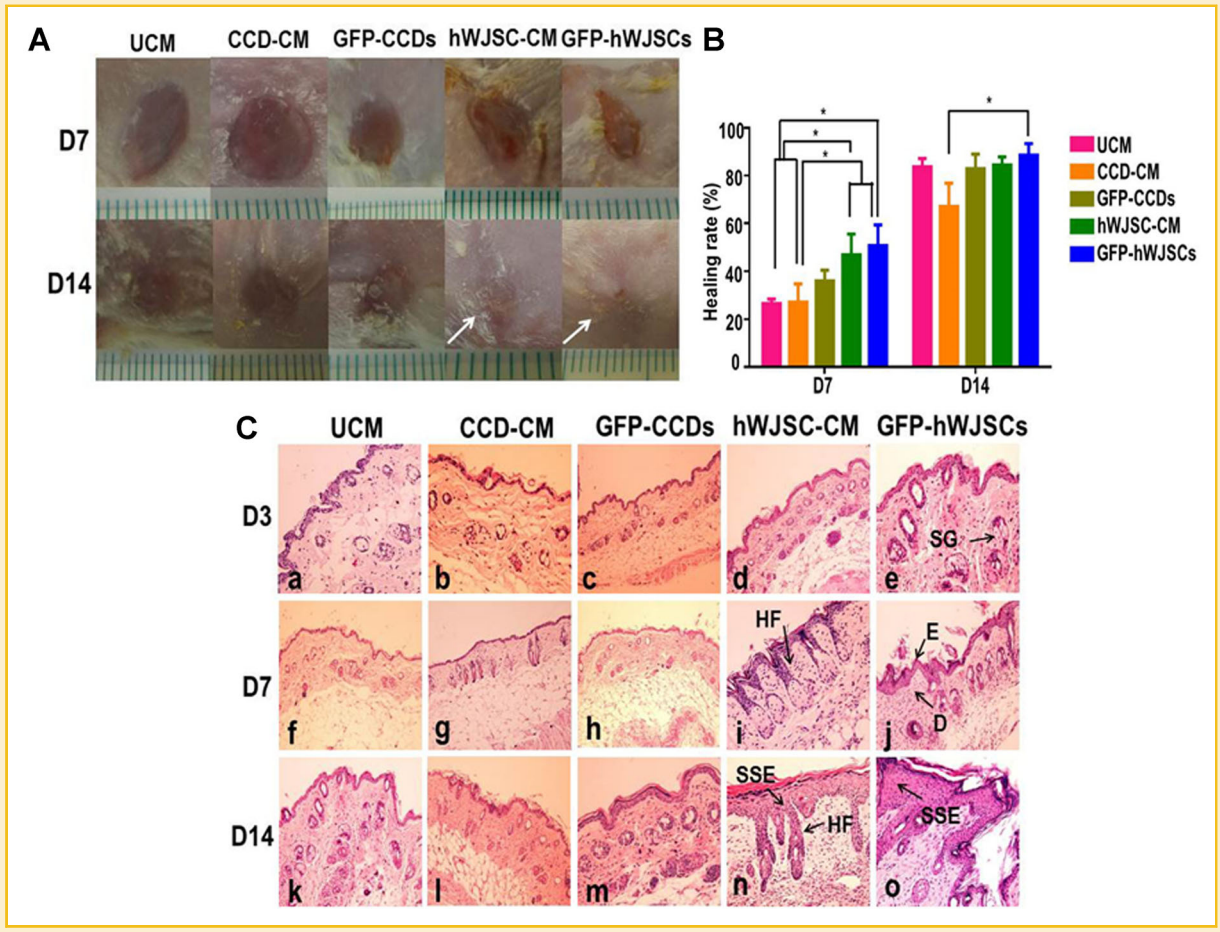


**Fig. 3.** A: Digital images of mouse excisional wounds showing faster wound closure by 14 days (D14) in SCID mice exposed to GFP-hWJSCs and hWJSC-CM (treatment arms) (white arrows) compared to controls (GFP-CCDs, CCD-CM and UCM). B: On day 7, mean ± SEM percentage healing rates in excisional wounds in SCID mice were significantly greater in the treatment arms (GFP-hWJSCs and hWJSC-CM) compared to controls ($^{*}P < 0.05$). On day 14, the mean ± SEM percentage healing rates were significantly greater for the GFP-hWJSCs treatment arm compared to controls ($^{*}P < 0.05$). C: Hematoxylin and eosin histological sections of murine wound biopsies taken at days 3, 7, and 14 (D3, D7, D14). On D14, the epidermis and dermis of wounds in the treatment groups (GFP-hWJSCs and hWJSC-CM) showed reepithelialization, formation of stratified squamous epithelium, increased cellularity and vasculature, and increased numbers of sebaceous glands and hair follicles when compared to the controls (n, o). On D7 even though healing rates were not 100% in the hWJSCs and hWJSC-CM treatments arms, some histological sections showed both dermal and epidermal layers suggesting that the healing process was rapid (i,j). D, dermis; E, epidermis; HF, hair follicle; SG, sebaceous gland; SSE, stratified squamous epithelium. Scale bar = 100 μm.

qRT-PCR and species-specific surface marker analysis on wound biopsies in the present study helped to discriminate between the presence of murine and human cells. The upregulation of ICAM-1, TIMP-1, and VEGF-A allowed us to hypothesize that both hWJSCs and hWJSC-CM modulate differential gene expression in the wounds bringing about cell adhesion, increased angiogenesis and epithelialization during wound healing. VEGF-A is unique for its multiple effects on the wound healing cascade such as angiogenesis, epithelialization, and collagen deposition [Bao et al., 2009]. ICAM-1 is central to the regulation of the inflammatory process during wound healing in the human and mouse [Yukami et al., 2007; Gay et al., 2011] because in the ICAM-1 knockout mouse model there was a delayed response to wound healing [Nagaoka et al., 2000]. Cytokine protein array analysis from our laboratory showed that important cytokines such as ICAM-1, IL-6, IL-8, and TIMP-1 were secreted in large concentrations by hWJSCs in 72 h hWJSC-CM compared to controls [Fong et al., 2012]. Such cytokines in the hWJSC-CM thus play a vital role in accelerating wound healing in the early phases. The hWJSCs secretome may help in jumpstarting the wound healing process and subsequent paracrine effects on endogenous mouse cytokine or growth factor secretion. Our qRT-PCR results demonstrated that the treatment of hWJSCs to wounds showed increased expression of mouse ICAM-1 and TIMP-1 as early as day 3. Also, the ICAM-1 mRNA results on day 14 strongly correlate with the observations of wound closure in vivo suggesting that hWJSCs may be producing adhesion molecules for the acceleration of wound closure during the early phases of wound healing. An increase of TIMP-1 mRNA expression observed on day 14 in CCD-CM treated wounds suggest that the delay in wound healing observed in the CCD-CM treated mice may be due to the late transcriptional upregulation of TIMP-1. Several published reports have also shown high levels of matrix metalloproteinases (MMPs) and low levels of tissue inhibitors

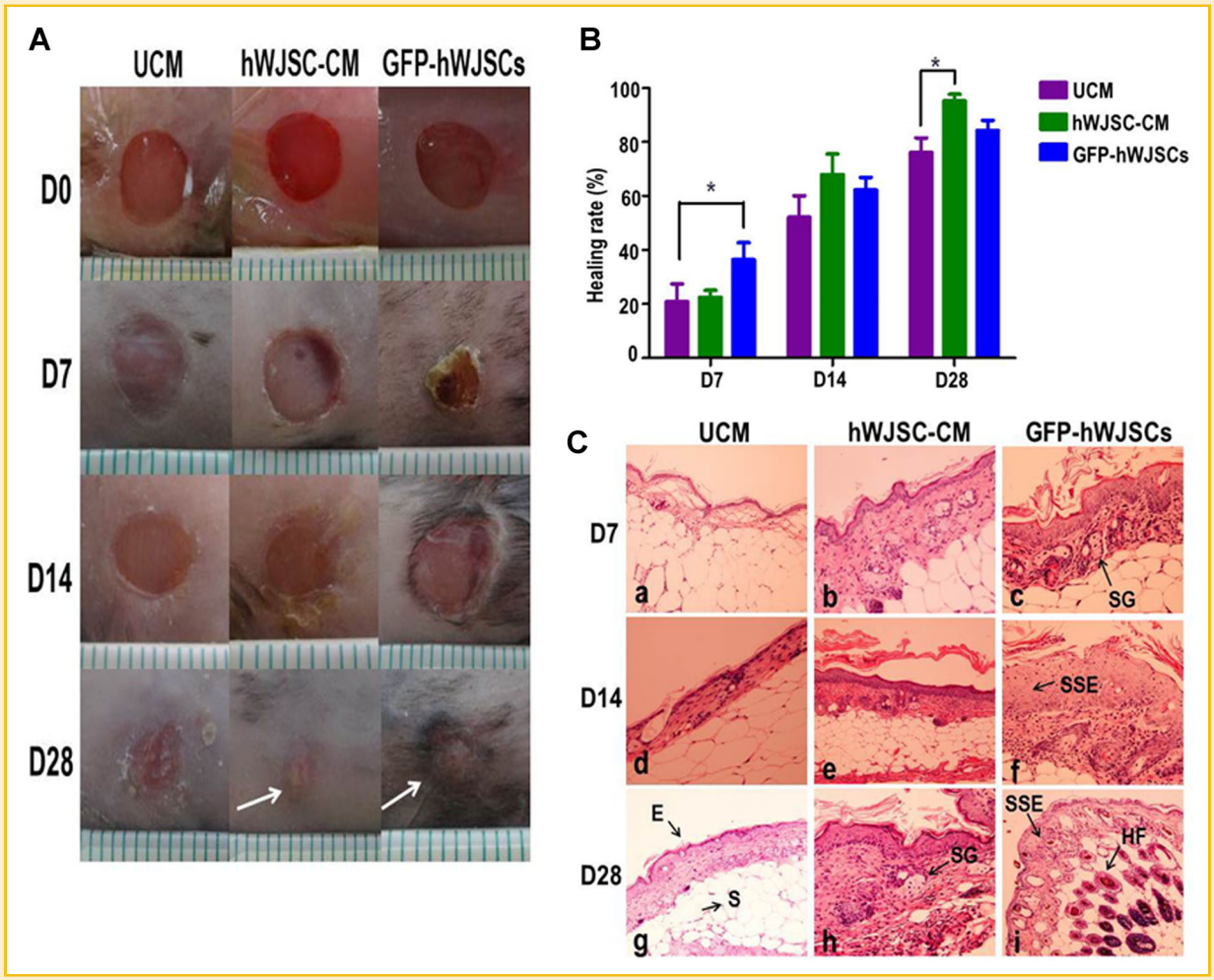


**Fig. 4.** A: Digital images of mouse diabetic wounds showing faster wound closure by 28 days (D28) in diabetic mice exposed to GFP-hWJSCs and hWJSC-CM (treatment arms) (white arrows) compared to controls (UCM). B: Mean ± SEM percentage healing rates in diabetic wounds in diabetic mice were significantly greater in the GFP-hWJSCs treatment arm on D7 and in the hWJSC-CM treatment arm on D28 compared to controls ($^{*}P < 0.05$). C: Hematoxylin and eosin histological sections of murine diabetic wound biopsies taken at days 7, 14, and 28 (D7, D14, D28). By D14 and D28, the epidermis of wound biopsies of the treatment arms (GFP-hWJSCs and hWJSC-CM) showed reepithelialization and formation of stratified squamous epithelium. The dermis showed increased cellularity and vasculature, and increased sebaceous gland and hair follicle numbers compared to the controls. E, epidermis; HF, hair follicle; SG, sebaceous gland; S, stroma; SSE, stratified squamous epithelium. Scale bar = 100 μm.

of MMPs (TIMPs) in chronic wound beds indicative of impaired wound healing [Liu et al., 2009; Stevens and Page-McCaw, 2012]. MMPs play a major role in wound healing as they can break down all components of the extracellular matrix (ECM) [Stevens and Page-McCaw, 2012]. In diabetic wounds there is a rise in MMPs and a decrease of TIMPs. High levels of MMP-1 are essential for wound healing while increased levels of MMP-8 and -9 are deleterious. The MMP-1/TIMP-1 ratio was considered a good predictor of healing of diabetic wounds [Muller et al., 2008]. It is interesting to note that in the present study high levels of secreted TIMP-1 was evident in hWJSC-CM at 72 h and was consistent on a transcriptional level with significant increases in gene expression of fibronectin, collagen I and III indicating that hWJSCs secrete endogenous proteins which affect ECM remodeling.

Collagen is normally produced during the inflammatory phase of wound healing and the ECM secreted by the dermal fibroblasts helps wound remodeling. Fathke et al. [2004] demonstrated that MSC populations produce collagen types I and III providing long-term reconstitution of the cutaneous wound. Collagen type III was also reported to be expressed in early healing processes of skin [Zhang et al., 1995]. The upregulation of collagen I and III by the CCDs following exposure to hWJSC-CM in the present study also suggests that hWJSC-CM supports wound healing. In the present study hWJSC-CM also stimulated increases in fibronectin and elastin. Fibronectin is another important ECM protein secreted by dermal fibroblasts during the proliferative phase of wound healing [Bielefeld et al., 2011] and is essential in providing the necessary mechanical strength to wounds [Clark, 1990]. Elastin confers the elasticity and resilience to the skin and these fibers are usually interwoven among collagen bundles. Elastin is also involved in cell signaling and migration in the wound healing process [Rnjak et al., 2011].

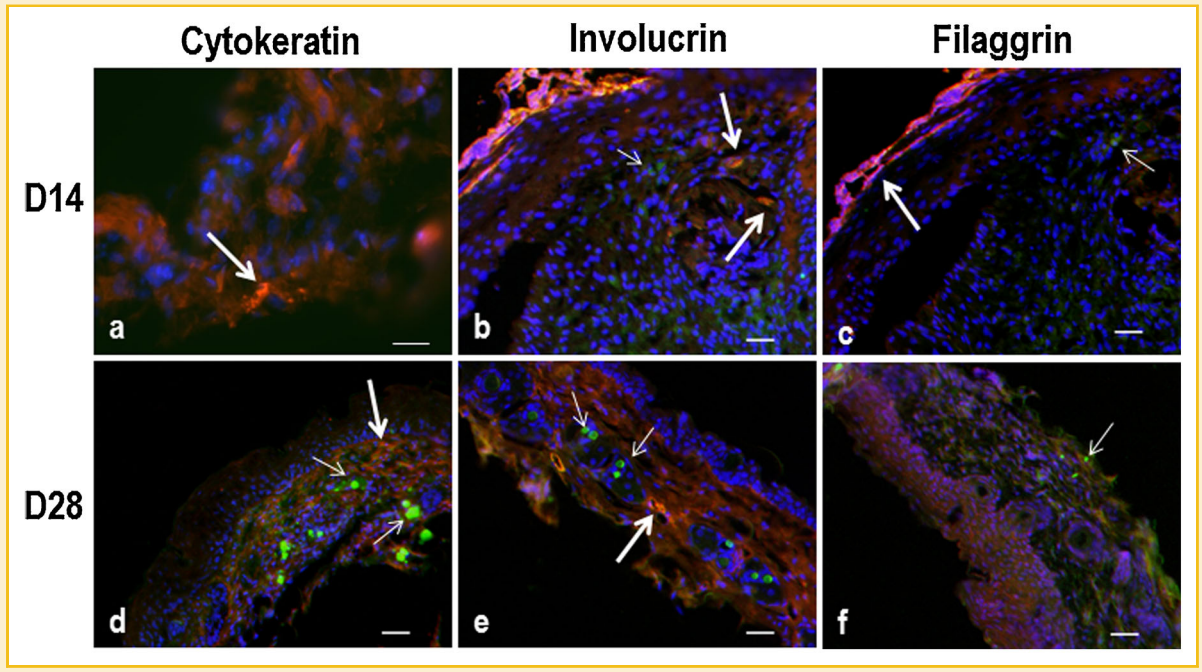


**Fig. 5.** Fluorescent immunohistochemical images of diabetic mouse wound biopsies on D14 and D28 showing green GFP-labeled hWJSCs (short thin arrows) and positive human keratinocyte markers (red) (thick long arrows). a,d: Represent cytokeratin clone AE1/AE3; (b,e) represent involucrin; and (c,f) represent filaggrin. DAPI: blue. Scale bar = 50 μm.

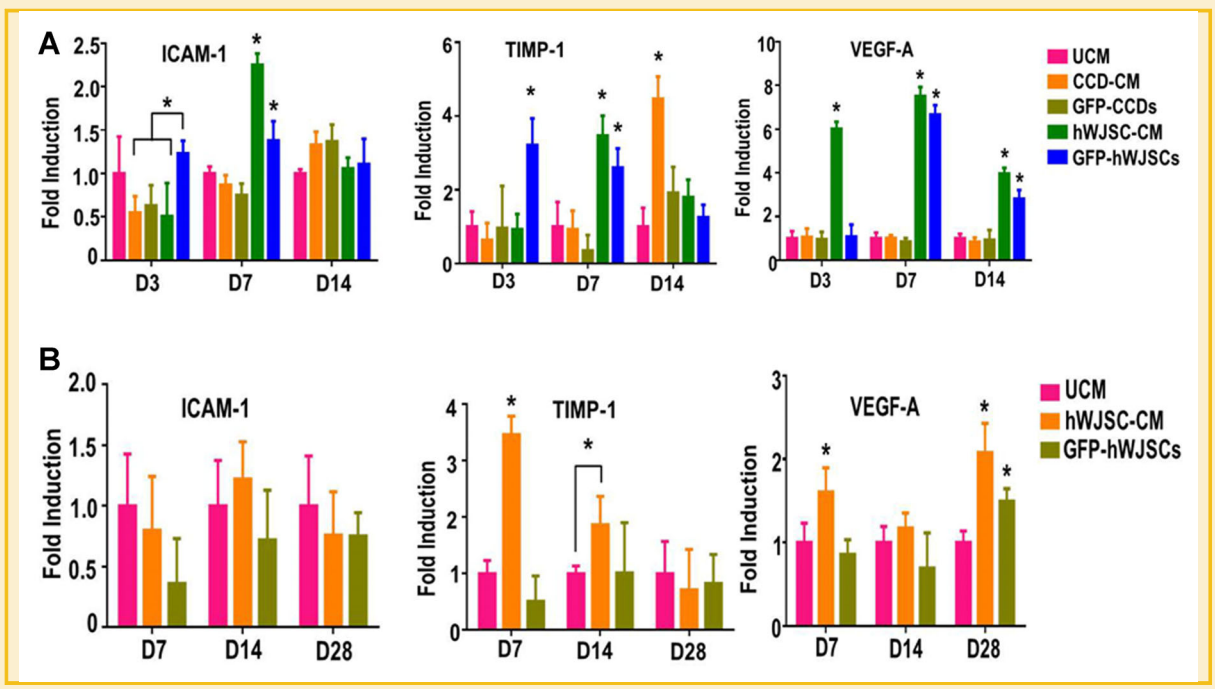


**Fig. 6.** qRT-PCR mRNA expression for mouse ICAM-1, TIMP-1 and VEGF-A using TaqMan probes in (A) excisional wound biopsies and (B) diabetic wound biopsies on days 3–28 (D3–D28). A: On D3 ICAM-1 mRNA levels in GFP-hWJSC treated excisional wounds were significantly higher than controls (CCD-CM and GFP-CCDs) ($^{*}P < 0.05$). TIMP-1 expression was also significantly upregulated in GFP-hWJSCs treated excisional wounds on D3 compared to controls ($^{*}P < 0.05$). VEGF-A mRNA expression on D3 showed a sixfold increase in hWJSC-CM treated excisional wounds compared to controls ($^{*}P < 0.05$). On D7, both GFP-hWJSCs and hWJSC-CM treated excisional wounds arms showed significantly greater ICAM-1, TIMP-1, and VEGF-A expression levels compared to controls ($^{*}P < 0.05$). On D14, ICAM-1 levels for excisional wounds were not significantly different between groups but VEGF-A levels were significantly greater in GFP-hWJSCs and hWJSC-CM treated excisional wounds compared to controls ($^{*}P < 0.05$). B: For diabetic wounds, the hWJSC-CM treatment arm showed significantly greater levels of TIMP-1 on D7 and D14 and VEGF-A on D7 and D28 compared to controls. VEGF-A levels for both the GFP-hWJSCs and hWJSC-CM arms were significantly greater than controls on D28 ($^{*}P < 0.05$).

TABLE II. Comparison of miRNA Expression in hWJSCs and CCDs

| hsa-miRNA | Average fold change | *P*-value | Function/ implication |
|---|---|---|---|
| let-7a-2-3p | 1.141 | 0.533 | Endothelial |
| let-7d | 1.077 | 0.651 | Endothelial |
| let-7e | 1.269 | 0.474 | Endothelial |
| let-7f | 2.061 | 0.453 | Endothelial |
| let-7f-1-3p | 1.088 | 0.845 | Endothelial |
| let-7g | 1.165 | 0.316 | Endothelial |
| let-7i | 1.087 | 0.301 | Endothelial |
| let-7i-3p | 1.164 | 0.541 | Endothelial |
| miR-100 | 1.125 | 0.499 | Endothelial |
| miR-106a | 2.501 | 0.075 | miR-106a-363 |
| miR-106b | 1.241 | 0.31 | miR-106b-25 |
| miR-125a-3p | 1.343 | 0.485 | Endothelial |
| miR-125a-5p | 1.078 | 0.819 | Endothelial |
| miR-126 | 16.957 | 0.523 | AngiomiRs, endothelial |
| miR-146a | 10.998 | 0.514 | Wound healing |
| miR-17 | 1.954 | 0.22 | miR-17-92 |
| miR-181a | 2.184 | 0.043 | Endothelial |
| miR-18b | 2.567 | 0.062 | miR-106a-363 |
| miR-196a-3p | 1.861 | 0.05 | |
| miR-19a | 1.771 | 0.157 | miR-17-92 |
| miR-19b | 2.011 | 0.062 | miR-17-92; miR-106a-363 |
| miR-200b | 1.229 | 0.434 | VEGF induced |
| miR-20a | 1.948 | 0.315 | miR-17-92; endothelial; angiomiRs |
| miR-20b | 2.985 | 0.199 | miR-106a-363; angiomiRs |
| miR-21 | 1.717 | 0.264 | Endothelial; angiomiRs |
| miR-210 | 1.748 | 0.346 | AngiomiRs; VEGF induced |
| miR-25 | 1.359 | 0.519 | miR-106b-25 |
| miR-27a-5p | 3.481 | 0.033 | |
| miR-29b | 1.114 | 0.854 | Pro-apoptotic |
| miR-302a | 1.013 | 0.741 | miR-302-367 |
| miR-302b-5p | 1.423 | 0.61 | miR-302-367 |
| miR-302c-5p | 1.016 | 0.913 | miR-302-367 |
| miR-30c | 1.137 | 0.568 | Endothelial |
| miR-31 | 1.078 | 0.822 | Endothelial; angiomiRs; VEGF induced |
| miR-32 | 1.343 | 0.684 | miR-25 homolog |
| miR-335 | 22.354 | 0.481 | AngiomiRs |
| miR-34a | 1.315 | 0.502 | Pro-apoptotic |
| miR-374a | 1.739 | 0.039 | |
| miR-378 | 1.638 | 0.371 | AngiomiRs |
| miR-3915 | 1.8 | 0.019 | |
| miR-3924 | 1.691 | 0.029 | |
| miR-601 | 2.882 | 0.044 | |
| miR-622 | 1.776 | 0.043 | |
| miR-920 | 4.199 | 0.002 | |
| miR-92a | 1.556 | 0.372 | miR-17-92 |
| miR-93 | 1.246 | 0.699 | miR-106b-25 |
| miR-98 | 1.515 | 0.006 | |

Total RNA was extracted from three different hWJSC lines and subjected to miRNA microarray analysis. Fold-change of miRNA expression was calculated with reference to CCD (hWJSC vs. CCD). Functional annotations of the respective miRNAs were extracted from the published data.

It has been suggested that bioactive molecules released by apoptotic cells stimulate endogenous native and engrafted exogenous MSCs in wounds to initiate the regenerative process of wound healing [Li et al., 2010]. Caspase 3/7 and prostaglandin E2 (PGE2) released from damaged apoptotic cells in wounds stimulate the MSCs at the damaged site to proliferate, differentiate, and eventually replace the damaged tissue ("Phoenix rising" pathway) [Li et al., 2010]. Mice lacking in these caspases were deficient in skin wound healing [Li et al., 2010]. More recent evidence confirmed the idea that dying cells signal their presence to the surrounding tissue and in doing so elicit repair and regeneration via stem or progenitor cells that compensate for any loss of function caused by cell death [Jager and Fearnhead, 2012]. These molecules may play important roles in stimulating the hWJSCs applied to the wounds in the present study to enhance healing.

Specific miRNA clusters (miR-106a-363, miR-17-92, miR-106b-25, miR-302-367, and miR-21) were highly expressed in hWJSCs. The miR-106a-363 and miR-17-92 clusters that were overexpressed are involved in cell proliferation and growth thus possibly playing a role in the wound healing process. Functionally, miR-106b-25 promotes cell-cycle progression and hyperproliferation via inhibition of the pro-apoptotic genes such as *E2F1*, *Bim*, Fas-activated kinase, *CASP7*, and *PTEN*. Combined inhibition of pro-apoptotic genes further provides miR-106b-25-expressing cells with a survival and progression or proliferation benefit. MiR-106b-25 upregulation may lead to enhanced binding to collagen therefore increasing ECM binding. The miR-302-367 cluster targets *TGF*β receptor 2 to increase E-cadherin expression and accelerates mesenchymal-to-epithelial transition [Liao et al., 2011]. This cluster may be involved in the enhanced reepithelialization in the wounds in the present study. In the normal wound healing process miR-21 is upregulated on day 8 and downregulated in diabetic wounds [Madhyastha et al., 2012]. MiR-21 exhibits a dual function (proliferative and anti-apoptosis) on vascular smooth muscle cells (VSMCs) [Ji et al., 2007]. The role of apoptotic miRNA in promoting tissue regeneration in wound healing was emphasized by Li et al. [2010] in their "Phoenix rising" mechanism of wound healing. The *VEGF*-induced miRNAs (miR-191, -155, -31, -17-5p, -18a, and -20a) [Suarez et al., 2008] were also significantly upregulated in hWJSCs compared to CCDs and hBMMSCs. VEGF is an important player in the wound healing process [Bao et al., 2009]. Based on our microarray data analysis, besides, the specific miRNAs that have been found to be involved in proliferation, wound healing and pro-angiogenic processes (Table II), the miRNAs belonging to the clusters described above were also significantly overexpressed in hWJSCs. Thus, the enhanced wound healing observed in the presence of hWJSCs and hWJSC-CM is probably guided by several miRNAs that provide beneficial effects to the wound healing process.

## REFERENCES


Badiavas EV, Abedi M, Butmarc J, Falanga V, Quesenberry P. 2003. Participation of bone marrow derived cells in cutaneous wound healing. J Cell Physiol 196:245–250.

Bao P, Kodra A, Tomic-Canic M, Golinko MS, Ehrlich HP, Brem H. 2009. The role of vascular endothelial growth factor in wound healing. J Surg Res 153:347–358.

Bey E, Prat M, Duhamel P, Benderitter M, Brachet M, Trompier F. 2010. Emerging therapy for improving wound repair of severe radiation burns using local bone marrow-derived stem cell administrations. Wound Repair Regen 18:50–58.

Bielefeld KA, Amini-Nik S, Whetstone H, Poon R, Youn A, Wang J. 2011. Fibronectin and β-catenin act in a regulatory loop in dermal fibroblasts to modulate cutaneous healing. J Cell Biochem 286:27687–27697.

Bongso A, Fong CY. 2013. The therapeutic potential, challenges and future clinical directions of stem cells from the Wharton′s jelly of the human umbilical cord. Stem Cell Rev Rep 9:226–240.

Borue X, Lee S, Grove J, Herzog EL, Harris R, Diflo T. 2004. Bone marrow-derived cells contribute to epithelial engraftment during wound healing. Am J Pathol 165:1767–1772.

Chen L, Tredget EE, Liu C, Wu Y. 2009. Analysis of allogenecity of mesenchymal stem cells in engraftment and wound healing in mice. PLoS ONE 4:e7119.

Clark RAF. 1990. Fibronectin matrix deposition and fibronectin receptor expression in healing and normal skin. J Invest Dermatol 94:128S–134S.

Cory G. 2011. Scratch-wound assay. Methods Mol Biol 769:25–30.

Dominici M, Le Blanc K, Mueller I, Slaper-Cortenbach I, Marini F, Krause D. 2006. Minimal criteria for defining multipotent mesenchymal stromal cells. The International Society for Cellular Therapy position statement. Cytotherapy 8:315–317.

Estes JM, Adzick NS, Harrison MR, Longaker MT, Stern R. 1993. Hyaluronate metabolism undergoes an ontogenic transition during fetal development: Implications for scar-free wound healing. J Pediatr Surg 28:1227–1231.

Fan CG, Zhang Q, Zhou J. 2011. Therapeutic potentials of mesenchymal stem cells derived from human umbilical cord. Stem Cell Rev Rep 7:195–207.

Fathke C, Wilson L, Hutter J, Kapoor V, Smith A, Hocking A. 2004. Contribution of bone marrow-derived cells to skin: Collagen deposition and wound repair. Stem Cells 22:812–822.

Fong CY, Richards M, Manasi N, Biswas A, Bongso A. 2007. Comparative growth behaviour and characterization of stem cells from human Wharton′s jelly. Reprod BioMed Online 15:708–718.

Fong CY, Subramanian A, Biswas A, Gauthaman K, Srikanth P, Hande MP, Bongso A. 2010. Derivation efficiency, cell proliferation, frozen–thaw survival, stem-cell properties, and differentiation of human Wharton′s jelly stem cells. Reprod BioMed Online 21:391–401.

Fong CY, Chak LL, Biswas A, Tan JH, Gauthaman K, Chan WK, Bongso A. 2011. Human Wharton′s jelly stem cells have unique transcriptome profiles compared to human embryonic stem cells and other mesenchymal stem cells. Stem Cell Rev Rep 7:1–16.

Fong CY, Gauthaman K, Cheyyatraivendran S, Lin HD, Biswas A, Bongso A. 2012. Human umbilical cord Wharton′s jelly stem cells and its conditioned medium support hematopoietic stem cell expansion ex vivo. J Cell Biochem 113:658–668.

Gauthaman K, Fong CY, Suganya CA, Subramanian A, Biswas A, Choolani M. 2012. Extra-embryonic human Wharton′s jelly stem cells do not induce tumorigenesis, unlike human embryonic stem cells. Reprod Biomed Online 24:235–246.

Gay AN, Mushin OP, Lazar DA, Naik-Mathuria BJ, Ling Yu, Gobin A. 2011. Wound healing characteristics of ICAM-1 null mice devoid of all isoforms of ICAM-1. J Surg Res 171:e1–e7.

Harris DT, Hilgaertner J, Simonson C, Ablin RJ, Badowski M. 2012. Cell-based therapy for epithelial wounds. Cytotherapy 14:802–810.

Jackson WM, Nesti LJ, Tuan RS. 2012. Concise review: Clinical translation of wound healing therapies based on mesenchymal stem cells. Stem Cells Transl Med 1:44–50.

Jager R, Fearnhead HO. 2012. Dead cells talking: The silent form of cell death is not so quiet. Biochem Res Int, doi: 10.1155/2012/453838

Jeon YK, Jang YH, Yoo DR, Kim SN, Lee SK, Nam MJ. 2010. Mesenchymal stem cells interaction with skin: Wound-healing effect on fibroblast cells and skin tissue. Wound Repair Regen 18:655–661.

Ji R, Cheng Y, Yue J, Yang J, Liu X, Chen H. 2007. MicroRNA expression signature and antisense-mediated depletion reveal an essential role of MicroRNA in vascular neointimal lesion formation. Circ Res 100:1579–1588.

Jin G, Prabhakaran MP, Ramakrishna S. 2011. Stem cell differentiation to epidermal lineages on electrospun nanofibrous substrates for skin tissue engineering. Acta Biomater 7:3113–3122.

Karolina DS, Armugam A, Tavintharan S, Wong M, Lim SC, Sum CF. 2011. MicroRNA 144 impairs insulin signaling by inhibiting the expression of insulin receptor substrate 1 in type 2 diabetes mellitus. PLoS ONE 6:e22839.

Kim SW, Zhang HZ, Guo L, Kim JM, Kim MH. 2012. Amniotic mesenchymal stem cells enhance wound healing in diabetic NOD/SCID mice through high angiogenic and engraftment capabilities. PLoS ONE 7:e41105.

Kuo YR, Wang CT, Cheng JT, Wang FS, Chiang YC, Wang CJ. 2011. Bone marrow-derived mesenchymal stem cells enhanced diabetic wound healing through recruitment of tissue regeneration in a rat model of streptozotocin-induced diabetes. Plast Reconstr Surg 128:872–880.

La Rocca G, Anzalone R, Corrao S, Magno F, Loria T, Lo Iacono M. 2009. Isolation and characterization of OCT4+/HLA-G+ mesenchymal stem cells from the human umbilical cord matrix: Differentiation potential and detection of new markers. Histochem Cell Biol 131:267–282.

Li F, Huang Q, Chen J, Peng Y, Roop D, Bedford J. 2010. Apoptotic cells activate the 'Phoenix rising' pathway to promote wound healing and tissue regeneration. Sci Signal 3:ra13.

Liao B, Bao X, Liu L, Feng S, Zovoilis A, Liu W. 2011. MicroRNA cluster 302–367 enhances somatic cell reprogramming by accelerating a mesenchymal-to-epithelial transition. J Cell Biochem 286:17359–17364.

Liu Y, Min D, Bolton T, Nubé V, Twigg SM, Yue DK. 2009. Increased matrix metaloproteinase-9 predicts poor wound healing in diabetic foot ulcers. Diabetes Care 32:117–119.

Lorenz HP, Longaker MT, Perkocha LA, Jennings RW, Harrison MR, Adzick NS. 1992. Scarless wound repair: A human fetal skin model. Development 114:253–259.

Luo G, Cheng W, He W, Wang X, Tan J, Fitzgerald M. 2010. Promotion of cutaneous wound healing by local application of mesenchymal stem cells derived from human umbilical cord blood. Wound Repair Regen 18:506–513.

Nagaoka T, Kaburagi Y, Hamaguchi Y, Hasegawa M, Takehara K, Steeber DA. 2000. Delayed wound healing in the absence of intercellular adhesion molecule-1 or L-selectin expression. Am J Pathol 157:237–247.

Madhyastha R, Madhyastha H, Nakajima Y, Omura S, Maruyama M. 2012. MicroRNA signature in diabetic wound healing: Promotive role of miR-21 in fibroblast migration. Int Wound J 9:355–361.

Martin P, D′Souza D, Martin J, Grose R, Cooper L, Maki R. 2003. Wound healing in the PU.1 null mouse–Tissue repair is not dependent on inflammatory cells. Curr Biol 13:1122–1128.

Mathieu D, Linke JC, Wattel F. 2006. Non-healing wounds. In: Mathieu DE, editor. Handbook on hyperbaric medicine. Amsterdam, The Netherlands: Springer. pp 401–428.

Maxson S, Lopez EA, Yoo D, Danilkovitch-Miagkova A, Leroux MA. 2012. Concise review: Role of mesenchymal stem cells in wound repair. Stem Cells Transl Med 1:142–149.

Muller M, Trocme C, Lardy B, Morel F, Halimi S, Benhamou PY. 2008. Matrix metalloproteinases and diabetic foot ulcers: The ratio of MMP-1 to TIMP-1 is a predictor of wound healing. Diabet Med 25:419–426.

Pappa KI, Anagnou NP. 2009. Novel sources of fetal stem cells: Where do they fit on the developmental continuum? Future Med 4:423–433.

Rnjak J, Wise SG, Mithieux SM, Anthony S, Weiss AS. 2011. Severe burn injuries and the role of elastin in the design of dermal substitutes. Tissue Eng Part B Rev 17:81–91.

Sasaki M, Abe R, Fujita Y, Ando S, Inokuma D, Shimizu H. 2008. Mesenchymal stem cells are recruited into wounded skin and contribute to wound repair by transdifferentiation into multiple skin cell type. J Immunol 180:2581–2587.

Schneider RK, Püllen A, Kramann R, Bornemann J, Knüchel R, Neuss S. 2010. Long-term survival and characterisation of human umbilical cord-derived mesenchymal stem cells on dermal equivalents. Differentiation 79:182–193.

Shin L, Peterson DA. 2013. Human mesenchymal stem cell grafts enhance normal and impaired wound healing by recruiting existing endogenous tissue stem/progenitor cells. Stem Cells Transl Med 2:33–42.

Stevens LJ, Page-McCaw A. 2012. A secreted MMP is required for reepithelialisation during wound healing. Mol Biol Cell 23:1068–1079.

Stoff A, Rivera AA, Sanjib Banerjee, Moore N, Michael ST, Numnum T, Espinosa-de-Los-Monteros A. 2009. Promotion of incisional wound repair by human mesenchymal stem cell transplantation. Exp Dermatol 18:362–369.

Suarez Y, Hernando CF, Yu J, Gerber S, Harrison K, Pober J. 2008. Dicer-dependent endothelial microRNAs are necessary for postnatal angiogenesis. Proc Natl Acad Sci USA 105:14082–14087.

Sullivan SR, Underwood RA, Gibran NS, Sigle RO, Usui ML, Carter WG. 2004. Validation of a model for the study of multiple wounds in the diabetic mouse (db/db). Plast Reconstr Surg 113:953–960.

Taghizadeh RR, Cetrulo KJ, Cetrulo CL. 2011. Wharton′s jelly stem cells: Future clinical applications. Placenta 32:S311–S315.

Troyer DL, Weiss ML. 2008. Concise review: Wharton′s jelly-derived cells are a primitive stromal cell population. Stem Cells 26:591–599.

Walter MN, Wright KT, Fuller HR, MacNeil S, Johnson WE. 2010. Mesenchymal stem cell-conditioned medium accelerates skin wound healing: An in vitro study of fibroblast and keratinocyte scratch assays. Exp Cell Res 316:1271–1281.

Wang XY, lan Y, He WY, Zhang L, Yao HY, Hou C. 2008. Identification of mesenchymal stem cells in aorta-gonad-mesonephros and yolk sac of human embryos. Blood 111:2436–2443.

Wang Y, Han ZB, Ma J, Zuo C, Geng J, Gong W. 2012. A toxicity study of multiple-administration human umbilical cord mesenchymal stem cells in cynomolgus monkeys. Stem Cells Dev 21:1401–1408.

Wu Y, Chen L, Scott PG, Tredget EE. 2007. Mesenchymal stem cells enhance wound healing through differentiation and angiogenesis. Stem Cells 25:2648–2659.

Yukami T, Hasegawa M, Matsushita Y, Fujita T, Matsushita T, Horikawa M. 2007. Endothelial selectins regulate skin wound healing in cooperation with L-selectin and ICAM-1. J Leukoc Biol 82:519–531.

Zhang K, Garner W, Cohen L, Rodriguez J, Phan S. 1995. Increased Types I and III collagen and transforming growth factor- 1 mRNA and protein in hypertrophic burn scar. J Investig Dermatol 104:750–754.